

Structural and electrical properties of $y(\text{Ni}_{0.7}\text{Co}_{0.2}\text{Cd}_{0.1}\text{Fe}_2\text{O}_4) + (1-y)\text{Ba}_{0.9}\text{Sr}_{0.1}\text{TiO}_3$ magnetoelectric composite

R K Pinjari¹, B A Aldar¹, N M Burange^{1*} & C H Bhosale²

¹Department of Physics, Smt Kasturbai Walchand College, Sangli 416 416, India

²Department of Physics, Shivaji University, Kolhapur, 416 004, India

Received 19 May 2014; revised 14 July 2014; accepted 6 January 2015

Magnetoelectric (ME) composites of ferrite and ferroelectric phase with $y(\text{Ni}_{0.7}\text{Co}_{0.2}\text{Cd}_{0.1}\text{Fe}_2\text{O}_4) + (1-y)\text{Ba}_{0.9}\text{Sr}_{0.1}\text{TiO}_3$ with $y=0.15, 0.30$ and 0.45 , respectively were prepared by standard double sintering ceramic method. The constituent phases, i.e., ferrite and ferroelectric phase presence were confirmed by X-ray diffraction pattern. Scanning electron micrographs were studied to understand microstructure of the prepared samples. The dielectric constant (ϵ) and loss tangent ($\tan\delta$) were measured as a function of frequency and also function of temperature at the fixed frequencies 1, 10, 100 kHz and 1 MHz. The AC conductivity was studied to understand conduction mechanism.

Keywords: Magnetoelectric (ME) composite, Microstructure, Resistivity, Dielectric constant, Loss tangent, Conduction

1 Introduction

Magnetoelectric (ME) composite consists of magnetostrictive and piezoelectric phase. In ME composites, magnetic field induces electric polarization and electric field induces magnetization. Due to this convertibility, ME composites have large technological applications, such as transducers, data storage device and sensors¹⁻⁸. Such type of ME convertibility depends upon the coupling strength between magnetostrictive phase and piezoelectric phase⁹. Generally, magnetoelectric materials are divided into two categories: single phase and composites. Single phase materials are not suitable for practical application as it possesses weak magnetoelectric coefficient while composite consists of high magnetoelectric coefficient at room temperature.

In the present work, nickel cobalt cadmium is selected as a ferrite phase and barium strontium titanate as a ferroelectric phase. Previous study shows that addition of cadmium in nickel cobalt ferrite decreases Curie temperature¹⁰ and strontium in barium titanate increases dielectric constant¹¹. The aim of present work is to study structural, electrical and dielectric properties of $y(\text{Ni}_{0.7}\text{Co}_{0.2}\text{Cd}_{0.1}\text{Fe}_2\text{O}_4) + (1-y)\text{Ba}_{0.9}\text{Sr}_{0.1}\text{TiO}_3$ ME composites.

2 Materials and Methods

The ferrite phase was prepared using AR grade carbonates of nickel, cobalt, cadmium and iron oxide. These compositions were mixed and grounded in agate mortar for two hours and pre-sintered at 950°C for 12 h. The ferroelectric phases were also prepared by using same procedure by using barium carbonate, strontium carbonate and titanium oxide in appropriate molar proportions and pre-sintered at 1100°C for 12 h. The ME composites were prepared by mixing 15%, 30% and 45% of ferrite phase with 85%, 70% and 55% of ferroelectric phase, respectively. These composite mixtures were pre-sintered at 1150°C for 12 h. The pellets of these composite, having thickness of 2-3 mm and diameter of 10 mm, was prepared using hydraulic press. These pellets and composite powder were finally sintered at 1200°C for 12 h.

The constituent phases in ME composite, i.e., ferrite phase and ferroelectric phase were confirmed by X-ray diffraction technique by using Cu-K α radiation ($\lambda=1.5418 \text{ \AA}$). The average grain size was determined by SEM micrographs. DC resistivity (ρ) is determined by two probe method within the temperature range (30-850°C). The dielectric constant (ϵ) and loss tangent ($\tan\delta$) were determined by measuring capacitance and dielectric loss at room temperature as well as a function of temperature for the fixed frequency of 1, 10, 100 kHz, 1 MHz using the Hioki 3532-50 LCR Hi-Tester.

*Corresponding author (E-mail: nmburange@gmail.com)

3 Results and Discussion

Figure 1 represents X-ray diffraction patterns of $y(\text{Ni}_{0.7}\text{Co}_{0.2}\text{Cd}_{0.1}\text{Fe}_2\text{O}_4) + (1-y)\text{Ba}_{0.9}\text{Sr}_{0.1}\text{TiO}_3$ ME composite with $y = 0.0, 0.15, 0.30, 0.45,$ and 1.0 . From the figure, it is observed that all XRD patterns exhibit the characteristic peaks of both phases, i.e., (311) for ferrite phase and (110) for ferroelectric phase and hence, confirms the presence of both phases. Comparative study shows that the intensity of ferrite phase increases while those of ferroelectric decreases with increase in ferrite content which confirms law of mixture. The lattice parameters were calculated after further analysis. The lattice parameter of nickel cobalt cadmium ferrite was found to be $a=8.37 \text{ \AA}$ and that of ferroelectric $a=3.99 \text{ \AA}$ and $c=4.03 \text{ \AA}$. The lattice parameters of all composites are shown in Table 1.

Figure 2 shows SEM micrographs of the ME composites. The average grain sizes were calculated by using Cottrell's method. The average grain size of ferrite found $1.46 \mu\text{m}$ and that of ferroelectric is $1.29 \mu\text{m}$. It is also observed that average grain size increases with increase in ferrite content, similar

results are obtained by Bammannavar and Naik¹². The average grain sizes of all samples are given in Table 1.

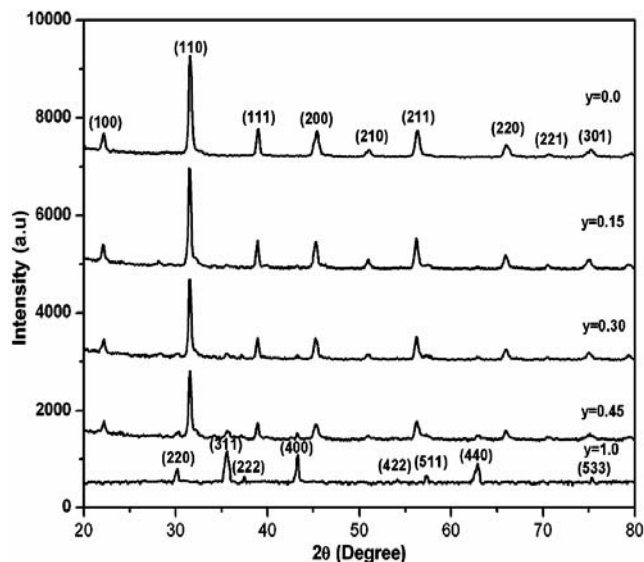


Fig. 1—XRD patterns of $y(\text{Ni}_{0.7}\text{Co}_{0.2}\text{Cd}_{0.1}\text{Fe}_2\text{O}_4) + (1-y)\text{Ba}_{0.9}\text{Sr}_{0.1}\text{TiO}_3$ ME composites

Table 1—Lattice parameter, average grain size, dc resistivity, activation energy of $y(\text{Ni}_{0.7}\text{Co}_{0.2}\text{Cd}_{0.1}\text{Fe}_2\text{O}_4) + (1-y)\text{Ba}_{0.9}\text{Sr}_{0.1}\text{TiO}_3$ ME composites

Composition	Lattice parameters (\AA)			Average grain size (μm)	$\rho_{\text{RT}} (\Omega \text{ cm}) \times 10^{10}$	Activation energy (eV)		Activation energy (eV) $\Delta E = E_p - E_f$	Curie temperature T_c ($^{\circ}\text{C}$)
	Ferrite	Ferroelectric	c/a			E_p	E_f		
y=0.0	-	a=3.99; c=4.03	1.01	1.29	19.2	0.69	0.041	0.649	60
y=0.15	8.37	a=4.00; c=4.02	1.004	1.11	8.9	0.879	0.095	0.784	830
y=0.30	8.37	a=4.01; c=4.04	1.009	1.19	5.03	0.891	0.093	0.798	800
y=0.45	8.37	a=4.01; c=4.02	1.003	1.26	2.5	0.896	0.087	0.809	770
y=1.0	8.37	-	-	1.46	0.9	0.879	0.116	0.763	730

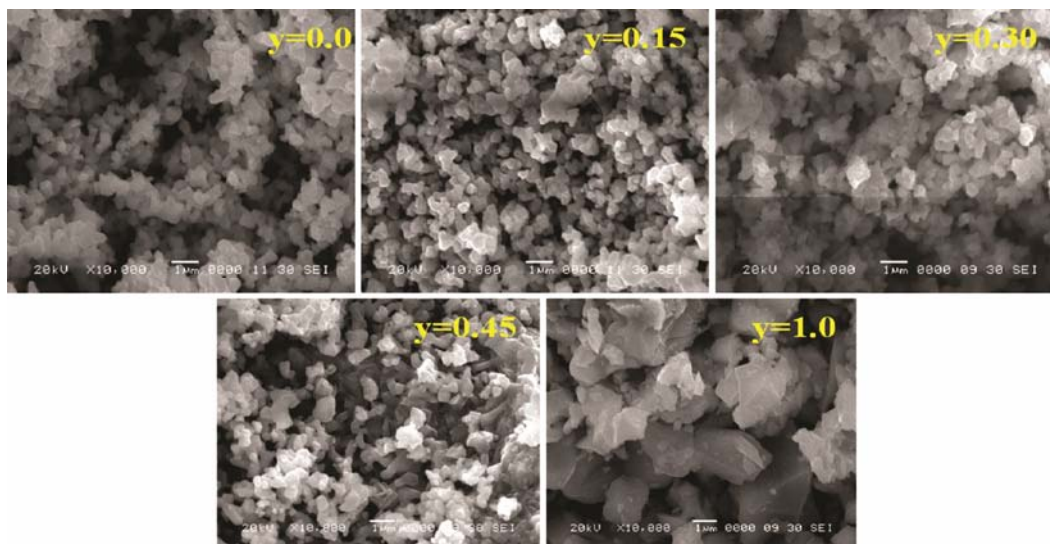


Fig. 2—SEM micrographs of $y(\text{Ni}_{0.7}\text{Co}_{0.2}\text{Cd}_{0.1}\text{Fe}_2\text{O}_4) + (1-y)\text{Ba}_{0.9}\text{Sr}_{0.1}\text{TiO}_3$ ME composites

Figure 3 shows the temperature dependent dc resistivity (ρ) of the composites. It is observed that ferroelectric phase has maximum resistivity than that of ferrite. It is also observed that the dc resistivity of ME composite decreases with increase in ferrite content, similar results were obtained by Lokare *et al.*¹³ and Kadam *et al.*¹⁴. For all samples, the plot shows the decrease in dc resistivity with increase in temperature and increase in ferrite content. The plot also shows two regions. The first region at low temperature is attributed to ferroelectric state while the second region at high temperature is attributed to para electric state due to thermally activated polaron hopping mechanism^{15,16}. By using Arrhenius relation, activation energies of all samples are calculated and listed in Table 1. For all the samples, activation energies are greater than 0.2 eV, which clearly indicates that the conduction is due to hopping of

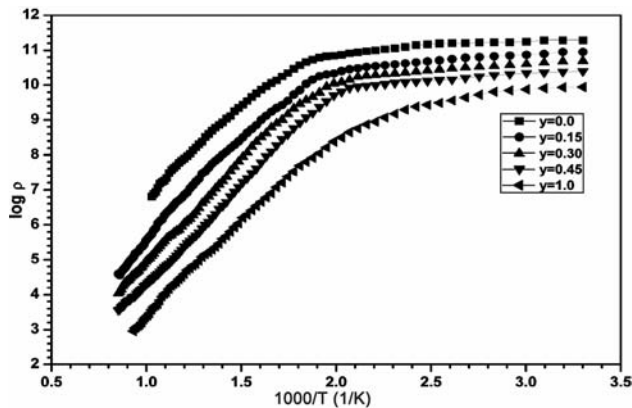


Fig. 3—Variation of DC resistivity with temperature for $y(\text{Ni}_{0.7}\text{Co}_{0.2}\text{Cd}_{0.1}\text{Fe}_2\text{O}_4)+(1-y)\text{Ba}_{0.9}\text{Sr}_{0.1}\text{TiO}_3$ ME composites

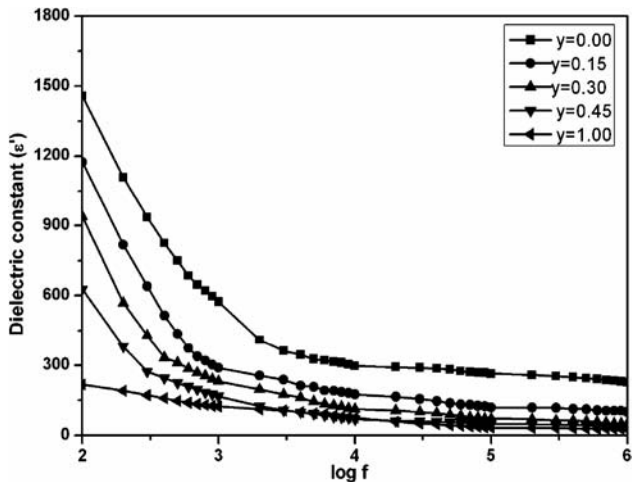


Fig. 4—Variation of dielectric constant (ϵ') with frequency for $y(\text{Ni}_{0.7}\text{Co}_{0.2}\text{Cd}_{0.1}\text{Fe}_2\text{O}_4)+(1-y)\text{Ba}_{0.9}\text{Sr}_{0.1}\text{TiO}_3$ ME composites

charge carriers. It is also observed that the activation energy increases with increase in ferrite content.

Figure 4 shows frequency dependence of dielectric constant. The plot shows decrease in dielectric constant with increase in frequency. At lower frequencies, dielectric constant decreases rapidly and attains a constant value at higher frequencies. The dielectric dispersion at lower frequencies is due to Maxwell Wagner type interfacial polarization^{17,18} in agreement with Koop's phenomenological theory¹⁹. At higher frequencies, the dielectric constant remains constant due to electronic polarization. It is also observed that with increase in ferrite content, dielectric constant decreases, which may be due to increase in conductivity²⁰. Figure 5 shows the variation of loss tangent with frequency. The plot shows similar behaviour as that of dielectric constant with frequency. The dielectric loss is the energy dissipation. At lower frequencies, dielectric loss ($\tan\delta$) is large and it decreases with increasing frequency. At higher frequencies, the losses are reduced and the dipoles contribute to the polarization. Similar dispersion is observed in the variation of dielectric loss as that of dielectric constant with frequency.

Figure 6 represents temperature dependence variation of dielectric constant of ME composite. For all samples, the dielectric constant is found to increase with increase in temperature, reaches a maximum value at Curie temperature and follow a decreasing trend, which indicates the phase transition. With the increase in temperature, the mobility of charge carrier's increases, which would lead to increase in

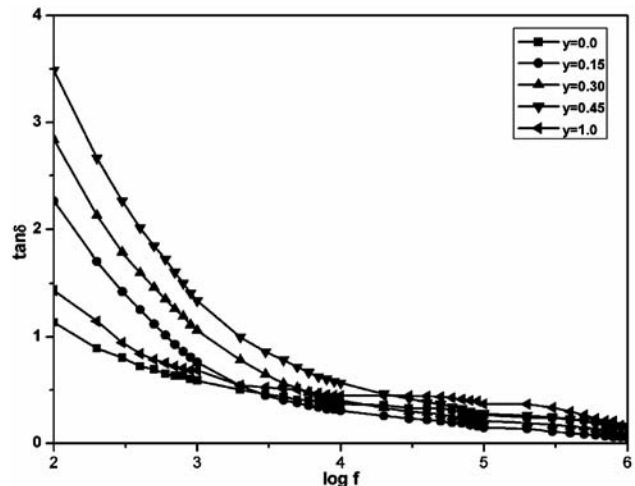


Fig. 5—Variation of loss tangent ($\tan\delta$) with frequency for $y(\text{Ni}_{0.7}\text{Co}_{0.2}\text{Cd}_{0.1}\text{Fe}_2\text{O}_4)+(1-y)\text{Ba}_{0.9}\text{Sr}_{0.1}\text{TiO}_3$ ME composites

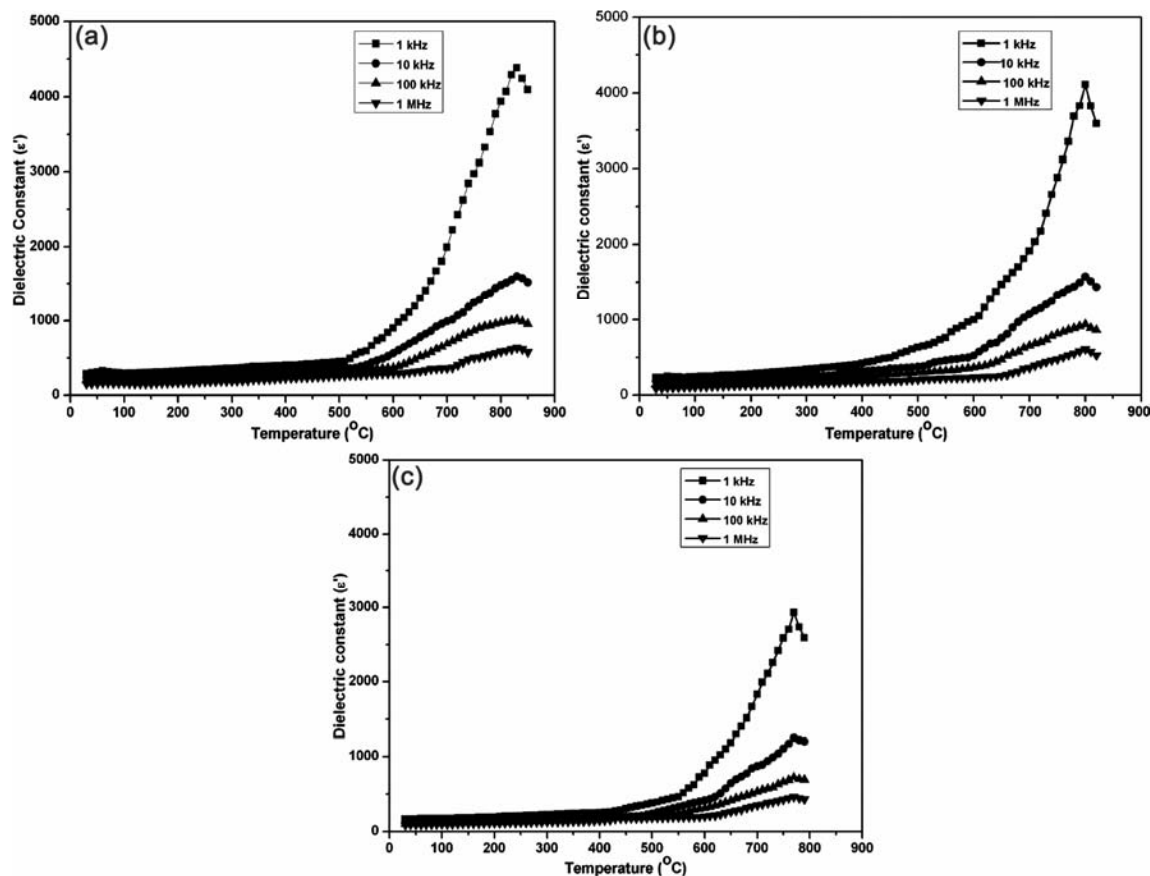


Fig. 6—Variation of dielectric constant (ϵ') with temperature for $y(\text{Ni}_{0.7}\text{Co}_{0.2}\text{Cd}_{0.1}\text{Fe}_2\text{O}_4)+(1-y)\text{Ba}_{0.9}\text{Sr}_{0.1}\text{TiO}_3$ ME composites with: (a) $y = 0.15$; (b) $y = 0.30$; and (c) $y = 0.45$

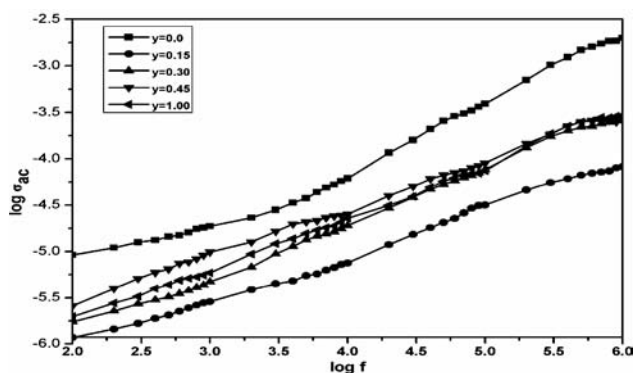


Fig. 7—Variation of AC conductivity with frequency for $\text{Ni}_{0.7}\text{Co}_{0.2}\text{Cd}_{0.1}\text{Fe}_2\text{O}_4+(1-y)\text{Ba}_{0.9}\text{Sr}_{0.1}\text{TiO}_3$ ME composites with $y = 0.0, 0.15, 0.30, 0.45, 1$.

polarization of the samples, hence, increase in dielectric constant. It is also found that with increase in ferrite content, Curie temperature shifts towards lower temperature region. The increase in ferrite content may also decrease the polarization efficiency and hence, decreases in dielectric constant due to increase in conductivity.

Figure 7 shows the variation of AC conductivity with frequency at room temperature. It is observed that AC conductivity increases with increase in frequency, which indicates small polaron type conduction²⁰.

4 Conclusions

ME composites with composition $y(\text{Ni}_{0.7}\text{Co}_{0.2}\text{Cd}_{0.1}\text{Fe}_2\text{O}_4)+(1-y)\text{Ba}_{0.9}\text{Sr}_{0.1}\text{TiO}_3$ were prepared by standard double sintering ceramic method and presence of phases was confirmed by XRD analysis. SEM micrographs show that the average grain size increases with increase in ferrite content. DC resistivity at higher temperature decreases exponentially indicating electron hopping conduction mechanism. The variation of the dielectric constant and the dielectric loss with frequency shows dispersion in the low frequency range. The dielectric constant is found to decrease with increasing ferrite content. Temperature dependence dielectric study shows that Curie temperature decreases with increase in ferrite content. The AC conductivity increases with

increase in frequency confirming small polaron hopping mechanism.

Acknowledgement

The authors are thankful to UGC, New Delhi for providing financial support for doing the research work under scheme of Major Research Project to College Teachers.

References

- 1 Cai N, *Solid State Phenom*, 111 (2006) 147.
- 2 Zhai Junyi, Xing Zengping, Dong Shuxiang, Li Jiefang & Viehland D, *Appl Phys Lett*, 88 (2006) 062510.
- 3 Bergs Richard, Islam Rashed A, Michael Vickers & Harry Stephanou & Priya Shashank, *J Appl Phys*, 101 (2007) 024108.
- 4 Nan C W & Clarke D R, *J Am Ceram Soc*, 80 (1997) 1333.
- 5 Ryu J, Priya S, Uchino K & Kim H E, *J Electroceram*, 8 (2002) 107.
- 6 Ping Li, Yumei Wen, Pangang Liu, Xinshen Li & Chaobo Jia, *Sens Actuat A*, 157 (2010) 100.
- 7 Yang Jin, Wena Yumei, Li Ping & Dai Xianzhi, *Sens Actuat A*, 168 (2011) 358.
- 8 Zhang Yihe, Zhou Jiayi, Wang Yu, Lai Helen & Chan Wa, *Int J Hydrogen Energy*, 38 (2013) 14915.
- 9 Harshe G, Dougherty J P & Newnham R E, *Int J Appl Electromagn Mater*, 4 (1993) 161.
- 10 Aldar B A, Pinjari R K & Burange N M, *IOSR J Appl Phys*, 6 (2014) 23.
- 11 Pinjari R K, Burange N M & Aldar B A, *Int J Eng Res Technol*, 3 (2014) 210.
- 12 Bammannavar B K & Naik L R, *J Magn Magn Mater*, 324 (2012) 944.
- 13 Lokare S A, Patil D R, Devan R S, Chougule S S, Kolekar Y D & Chougule B K, *Mater Res Bull*, 43 (2008) 326.
- 14 Kadam S L, Patanakar K K, Kanamadi C M & Chougule B K, *Mater Res Bull*, 39 (2004) 2265.
- 15 Lokare S A, Devan R S, Patil D R, Kolekar Y D, Patankar K K & Chougule B K, *J Mater Sci*, 42 (2007) 10250.
- 16 Mahajan R P, Patanakar K K, Burange N M, Chaudhari S C, Ghatage A K & Patil S A, *Indian J Pure Appl Phys*, 38 (2000) 615.
- 17 Maxwell J C, *Electricity and Magnetism* (Oxford University Press, London), 1973.
- 18 Wagner K W, *Ann Phys*, 40 (1993) 818.
- 19 Koop C G, *Phys Rev*, 83 (1951) 121.
- 20 Pandey D, Singh N & Mishra S K, *Indian J Pure Appl Phys*, 32 (1994) 616.
- 21 Klinger M I, *J Phys C*, (1975) 973 (D).